

Bound states of the generalized spiked harmonic oscillator

Amlan K. Roy*

*Department of Chemistry and Biochemistry,
University of California, Los Angeles, CA, 90095-1569, USA*

Abraham F. Jalbout

Institute of Chemistry, National Autonomous University of Mexico, Mexico City, Mexico

Abstract

Bound states of the generalized spiked harmonic oscillator potential are calculated accurately by using the generalized pseudospectral method. Energy eigenvalues, various expectation values, radial densities are obtained through a nonuniform, optimal spatial discretization of the radial Schrödinger equation efficiently. Ground and excited states corresponding to arbitrary values of n and ℓ are reported for potential parameters covering a wide range of interaction. Both weak and strong coupling is considered. The effect of potential parameters on eigenvalues and densities are discussed. Almost all of the results are reported here for the first time, which could be useful for future studies.

*Corresponding author. Email: akroy@chem.ucla.edu. Present address: Department of Chemistry, University of Kansas, Lawrence, KS, 66045, USA.

I. INTRODUCTION

The spiked harmonic oscillator (SHO) defined by the Hamiltonian $H = -d^2/dr^2 + r^2 + \lambda r^{-\alpha}$, where $r \in [0, \infty]$ and λ, α are positive definite parameters signifying the strength of perturbation and type of singularity, has been of considerable interest for over three decades. This has a number of interesting physical as well as mathematical properties and found applications in chemical, nuclear and particle physics. For example, this represents a prototype of the so-called Klauder phenomenon [1, 2], i.e., even after the perturbation is completely turned off ($\lambda \rightarrow 0$), some interaction still remains. The Rayleigh-Schrödinger perturbation series diverges following the relation $n \geq 1/(\alpha - 2)$, with n denoting the order of perturbation. Another interesting feature is that in the region of $\alpha \geq 5/2$, this gives rise to supersingularity, i.e., the potential is so singular that any nontrivial correction to the energy (matrix element) diverges [1]. A fascinating property from a purely mathematical point of view is that there is no dominance of either of the two terms r^2 and λ/r^α for the extreme values of λ . In other words, there is a tug-of-war between the two terms. Typical shape of the potential for a few parameter sets are depicted in Fig. 1

Like most of the practical physical systems, exact analytical solution of the corresponding Schrödinger equation (SE) for arbitrary parameters for a general state (both ground and excited) is yet to be known and consequently approximations such as variational or perturbation methods must be used. Thus a large number of attempts have been made towards the exact and approximate calculation of eigenvalues and eigenfunctions employing analytic, seminumerical or purely computational methods [3-18]. As the Rayleigh-Schrödinger perturbation series for the eigenvalues of the operator H diverges [3], a modified perturbation theory to finite order was developed which gave good result for the ground-state eigenvalues of small λ . For large positive values of λ , approximate estimates were made through the large coupling perturbative expansion [3]. A resummation technique for weak coupling of the nonsingular SHO ($\alpha < 5/2$) [4] was developed. Exact and approximate solutions are also given for the lowest states of a given angular momentum [6]. A WKB treatment has been proposed [11]. Recently extensive studies have been made on the upper and lower bounds as well as the direct eigenvalues by means of the geometrical approximation and method of potential envelopes [10, 12, 17]. The analytical pseudoperturbation shifted- ℓ expansion [14, 15] has also been suggested. Reliable results were reported by using a Richardson extrapolation

of the finite-difference scheme [16], integrating the radial Schrödinger equation by Lanczos grid method [8], analytic continuation method [9], etc. Recently a generalized pseudospectral (GPS) method was shown to produce very accurate results for the SHO eigenvalues, eigenfunctions and other properties [18]. Arbitrary eigenstates corresponding to any given n and ℓ values were treated for any general potential parameters within a simple and unified manner.

In parallel to these above works, recently there has been significant interest [19-24] in studying a *generalized spiked harmonic oscillator* (GSHO) as well, defined by the Hamiltonian,

$$H = -\frac{d^2}{dr^2} + v(r); \quad v(r) = r^2 + \frac{A}{r^2} + \frac{\lambda}{r^\alpha}, \quad A \geq 0 \quad (1)$$

both using variational and perturbation methods. Here λ , α are two real parameters and the SHO is a special case of GSHO with $A = 0$. The present study is motivated by these recent works of Hall and coworkers [19-24]. In [23] using a perturbation expansion up to 3rd order, they estimated the *lower and upper bounds* of the GSHO ground states for *small* coupling parameter λ (four values in the range of 0.001–1). However no *direct* results were given. Other than this, we are not aware of any other works towards the calculation of these bound states or even the approximate bounds. Hence it would be of some interest to investigate the spectra of this system in some detail. The objective of this work is thus to report the accurate eigenvalues, eigenfunctions, expectation values of some position operators of the GSHO for the first time. As shown in later sections, both *lower* and *higher* states can be tackled very efficiently for arbitrary parameters including both *weak* and *strong* coupling in a simple manner. Moreover, in order to understand the spectra, we make a detailed analysis on the effect of variation of the parameters on eigenvalues and radial densities. For this we employ the GPS method, which has been very successful to produce accurate and reliable results in recent years for a variety of singular potentials relevant to quantum mechanics, static and dynamic properties of atom, molecules, as well as the spherically confined isotropic harmonic oscillator [18,25-28]. The article is organized as follows: Section II gives a brief outline of the GPS method used here to solve the SE for the GSHO. A discussion of the results is made in Section III, while we make a few concluding remarks in Section IV.

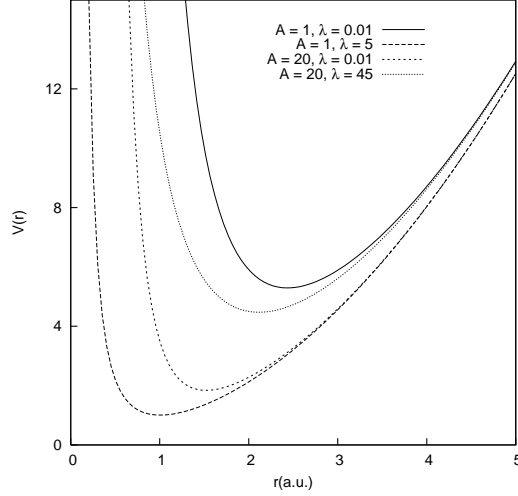


FIG. 1: The potential $V(r) = v(r)/2$, for $\alpha = 4$ for several values of A and λ .

II. METHOD OF CALCULATION

This section presents an overview of the GPS formalism used for solving the radial SE of a Hamiltonian containing a GSHO potential within the nonrelativistic framework. Only essential steps are given as relevant details have been presented earlier [18,25-28]. Unless otherwise mentioned, atomic units are employed throughout this Letter.

The radial SE can be written in the following form,

$$\left[-\frac{1}{2} \frac{d^2}{dr^2} + \frac{\ell(\ell+1)}{2r^2} + V(r) \right] \psi_{n,\ell}(r) = E_{n,\ell} \psi_{n,\ell}(r) \quad (2)$$

where $V(r) = v(r)/2$ and $v(r)$ is as given in Eq. (1). Note that a 2 factor is introduced for the sake of consistency with the literature. Here n and ℓ signify the usual radial and angular momentum quantum numbers respectively.

One of the distinctive features of GPS method is that it allows one to work in a nonuniform and optimal spatial discretization; a coarser mesh at larger r and a denser mesh at smaller r , while maintaining a similar accuracy at *both* the regions. Thus it suffices to work with a significantly smaller number of radial points efficiently, which is in sharp contrast to some of the commonly used finite difference or finite element methods for the singular potentials, where one is almost forced to use considerably larger mesh, often presumably because of their uniform nature. This feature was realized and exploited during the recent accurate calculation of high-lying multiply excited *Rydberg* series of Li isoelectronic series [25] using density functional theory.

The key step is to approximate a function $f(x)$ defined in the interval $x \in [-1, 1]$ by the N -th order polynomial $f_N(x)$ as follows through a cardinal function $g_j(x)$,

$$f(x) \cong f_N(x) = \sum_{j=0}^N f(x_j) g_j(x), \quad (3)$$

which guarantees that the approximation is *exact* at the *collocation points* x_j , i.e., $f_N(x_j) = f(x_j)$, requiring that the cardinal function satisfies $g_j(x_{j'}) = \delta_{j'j}$. In the Legendre pseudospectral method which we use here, $x_0 = -1$, $x_N = 1$, and the x_j ($j = 1, \dots, N-1$) are obtained from the roots of the first derivative of the Legendre polynomial $P_N(x)$ with respect to x as $P'_N(x_j) = 0$. The $g_j(x)$ are given by,

$$g_j(x) = -\frac{1}{N(N+1)P_N(x_j)} \frac{(1-x^2) P'_N(x)}{x-x_j}, \quad (4)$$

Now one can map the semi-infinite domain $r \in [0, \infty]$ onto the finite domain $x \in [-1, 1]$ by the transformation $r = r(x)$. At this stage, introduction of an algebraic nonlinear mapping,

$$r = r(x) = L \frac{1+x}{1-x+\gamma}, \quad (5)$$

where L and $\gamma = 2L/r_{max}$ are the mapping parameters, gives rise to the transformed differential equation as: $f(x) = R_{nl}(r(x))/\sqrt{r'(x)}$. Applying the Legendre pseudospectral method now to this equation followed by a symmetrization procedure finally leads to a *symmetric* eigenvalue problem,

$$\sum_{j=1}^{N-1} \left[-\frac{1}{2} D_{ij} + u_j \delta_{ij} \right] \chi_j = \epsilon_{nl} \chi_i \quad (6)$$

which can be easily solved by standard available routines to yield highly accurate eigenvalues and eigenfunctions. Here

$$\chi_i = R_{nl}(r_i) \sqrt{(r'_i)/P_N(x_i)}, \quad u_i = l(l+1)/2r_i^2 + v(r_i) \quad (7)$$

with $\chi_i = \chi(x_i)$, $u_i = u(x_i)$, $r_i = r(x_i)$, $r'_i = r'(x_i)$, and D_{ij} denoting the symmetrized second derivative of the cardinal function given as [18,25-28].

$$\begin{aligned} D_{ij} &= -\frac{2}{r'_i(x_i - x_j)^2 r'_j}, \quad i \neq j, \\ &= -\frac{N(N+1)}{3r_i'^2(1-x_i^2)}, \quad i = j. \end{aligned} \quad (8)$$

A large number of tests were carried out in order to make a detailed check on the accuracy and reliability of our calculation by varying the mapping parameters so as to produce “stable” results. In this way, a consistent set of parameters $\gamma = 25$, $N = 200$ and $r_{max} = 300$

were chosen which seemed to be appropriate for all the calculations performed in this work. The results are reported only up to the precision that maintained stability. The energy values are *truncated* rather than *rounded-off* and thus may be considered as correct up to the place they are reported.

III. RESULTS AND DISCUSSION

First in Table I we give a comparison of the GPS eigenvalues of GSHO with the available literature data as an illustration to assess the validity and usefulness of our present calculation. Lowest two eigenvalues of $\ell = 0, 1, 2, 3$ are given at six values of λ in the range of 0.001–100 covering both weaker and stronger interaction to demonstrate the generality of our results. The only result available in the literature corresponds to $A = 12$, $\alpha = 4$ and we stick to them, although we are confident that this will produce equally correct results for any other set of parameters or states. The lowest state corresponding to $\ell = 0$ for $\lambda = 0.001, 0.1, 0.1$ and 1 have been studied through the upper and lower bounds [23], and those are presented in the footnote. Note that those results are divided by 2 to get the entries in the table. They used a third-order perturbation expansion using the procedure suggested by Burrows et al [29]. As pointed out in [23], there are a number of variational methods available for the GSHO Hamiltonian, which can provide accurate *upper* bounds in question, but they do not lead to *direct* evaluation of energies. Furthermore, for *smaller* λ values, these methods are slow and in general, a large number of matrix elements are required to achieve a reasonable accuracy. As can be seen from the table, our results give estimates for all the four values of λ that perfectly lie in between those bounds. Clearly as anticipated, for smaller λ values the bounds are narrow and hence very accurate methods such as the present ones would be needed to generate correct values. No results are available for any other parameter sets or states and our calculation could be helpful in future studies of these systems. We also did similar calculations for $\alpha = 6$ with $A = 12$ leading to similar kind of results and conclusions and thus are omitted.

Next we consider the variation of eigenvalues of the GSHO through a cross-section of the sampled results for a varied range of representative parameter sets and states in Table II. For this, we choose four values of λ lying within the broad range of 0.005–50. For each λ , three values of A are selected, namely 5, 15 and 25 respectively. The angular quantum

TABLE I: Comparison of the calculated GSHO eigenvalues (in a.u.) for $A = 12$ and $\alpha = 4$. First two eigenvalues are given for each ℓ . Literature results are appropriately converted to the current scale of units.

λ	$\ell = 0$	$\ell = 1$	$\ell = 2$	$\ell = 3$
0.001	4.50005713955 ^a	4.77496494795	5.27203764224	5.92445477296
	6.50008253170	6.77498493821	7.27205121112	7.92446350670
0.01	4.50057109969 ^b	4.77539434151	5.27235948689	5.92468758726
	6.50082460262	6.77559400403	7.27249507610	7.92477488725
0.1	4.50568201308 ^c	4.77967076076	5.27556990359	5.92701233962
	6.50817676852	6.78164398019	7.27691597471	7.92788162240
1	4.55432930375 ^d	4.82086660209	5.30692177482	5.94993288816
	6.57618592946	6.83867710911	7.31951196183	7.95827867190
10	4.91961566042	5.14553963970	5.57091626978	6.15427959467
	7.03453114315	7.24781484749	7.65332837563	8.21617552368
100	6.54544524211	6.68956373653	6.9715527505	7.37986452167
	8.81244551008	8.94633479206	9.2093889489	9.59269153472

^aThe lower and upper bounds are 4.5000571155 and 4.5000571635 [23].

^bThe lower and upper bounds are 4.5005687045 and 4.5005734945 [23].

^cThe lower and upper bounds are 4.5054425485 and 4.5059217125 [23].

^dThe lower and upper bounds are 4.5306226410 and 4.5786886205 [23].

momentum ℓ is chosen at random from 0–3 and first two states belonging to each ℓ are given. We restrict ourselves to only two α values of 4 and 6, corresponding to the left and right panel respectively. No results have been reported so far in the literature for direct comparison and we hope these will inspire further works in future.

The above variation of energies with potential parameters are shown more clearly in Fig. 2. The top panel (a)–(c) depicts the λ vs. E plot for three A values, *viz.*, 5, 15, 25 respectively. For each A , the first three states of $\ell = 0$ are presented (E_1 , E_2 , E_3 from bottom to top) and λ varied from 0–35. These are studied for both $\alpha = 4$ and 6 as marked in the figure. Note that the energy axes in (a)–(c) and (d)–(f) are kept fixed at 0–12 and 2–13. The variation of energies with respect to λ are rather slow (monotonically increases as λ increases) for both $\alpha = 4$ and 6, with smaller α exerting relatively larger effect. At smaller λ (in the vicinity of zero), the $\alpha = 4$ and 6 energies are quite close to each other for all values of A and with an increase in λ they show pronounced separation. As A increases, the slope of λ vs. E decreases, making the plot rather flat as in (c), signifying even slower variation of E with respect to λ . In the bottom, we show the A vs. E in the range of $A = 5 - 50$

TABLE II: The calculated eigenvalues (in a.u.) of GSHO for various parameters. Left for $\alpha = 4$, right for $\alpha = 6$. Lowest two energies are given for each ℓ .

λ	A	ℓ	$\alpha = 4$		$\alpha = 6$	
			E_1	E_2	E_1	E_2
0.005	5	0	3.29213042081	5.29263961857	3.29301057259	5.29560957327
	15	0	4.90534516173	6.90543495986	4.90524031751	6.90538113434
	25	0	6.02506141110	8.02510243449	6.02497866843	8.02501934461
0.5	5	1	3.74338802444	5.76740985617	3.73736635296	5.78462712272
	15	1	5.17214026739	7.17923504322	5.16180870804	7.17100250031
	25	1	6.23143489376	8.23501549308	6.22364595141	8.22695053203
5	5	2	4.60929429358	6.69135284445	4.49045054121	6.59803098276
	15	2	5.74836543195	7.79050612724	5.66024910570	7.70391813910
	25	2	6.68350815067	8.70939627752	6.61603417371	8.63746955793
50	5	3	6.25457661591	8.44871213892	5.57496724850	7.79410043287
	15	3	7.03078249009	9.18083908970	6.46642800655	8.61050093425
	25	3	7.74063452037	9.85964537843	7.26355121587	9.36136024083

for three values of λ , namely 1, 10, 25 respectively in (d)–(f). Once again we show the first three states of $\ell = 0$ of both $\alpha = 4$ and 6, which make three separate families. For a given λ , as A increases, E increases rather sharply compared to those in top panel, (a)–(c). Interestingly however, for $\lambda = 1$, the $\alpha = 4$ and 6 plots seem to be virtually identical for all the three states. As λ increases the separation gradually increases slowly as one passes from (d)–(e)–(f).

Next in Fig. 3 we show the changes in ground-state radial probability distribution function $|rR_{n,l}|^2$ with respect to the potential parameters λ (a) and A (b) respectively. In (a) we fix A at 20 and four plots are given for $\lambda = 0.01, 50, 200$ and 500. With an increase in λ , the peak position and peak height shifts to higher values. In (b) we show the variation at four values of A (1, 10, 20 and 30) by keeping λ constant at 1. In this case, with an increase in A , the peak position increases, but the peak height decreases.

As a demonstration of the accuracy of our calculated wave functions, finally in Table III, two position expectation values $\langle r^{-1} \rangle$ and $\langle r \rangle$ (in a.u.) of the GSHO with $\lambda = 1$ and 10 are reported for $\alpha = 4$ (left) and 6 (right) respectively. First two states of $\ell = 0$ are given keeping A fixed at 20. There has been no result of these values for comparison.

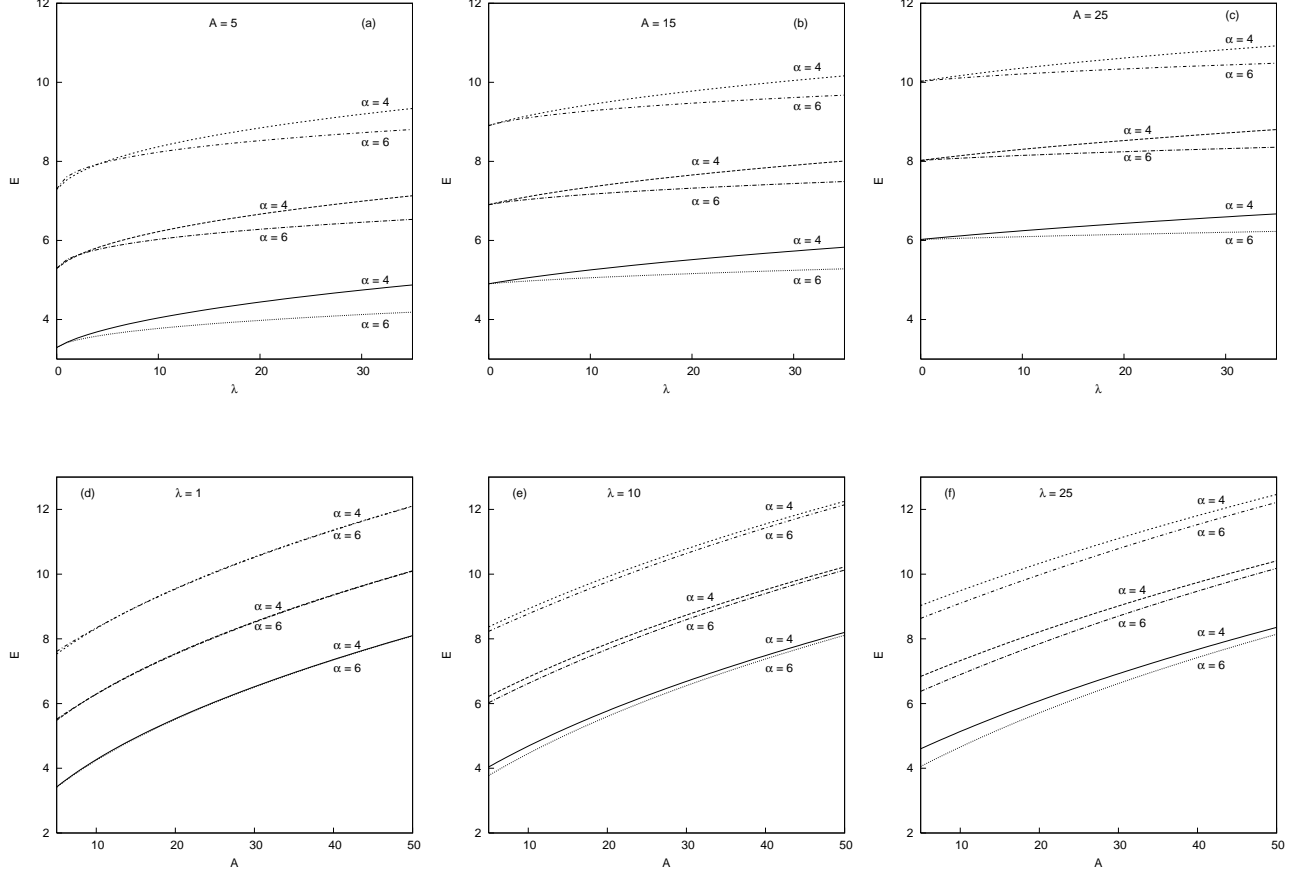


FIG. 2: Variation of E with respect to λ (top) and A (bottom) respectively for the first three states belonging to $\ell = 0$ of a GSHO having $\alpha = 4$ and 6. (a) $A = 5$, (b) $A = 15$, (c) $A = 25$; (d) $\lambda = 1$, (e) $\lambda = 10$, (f) $\lambda = 25$.

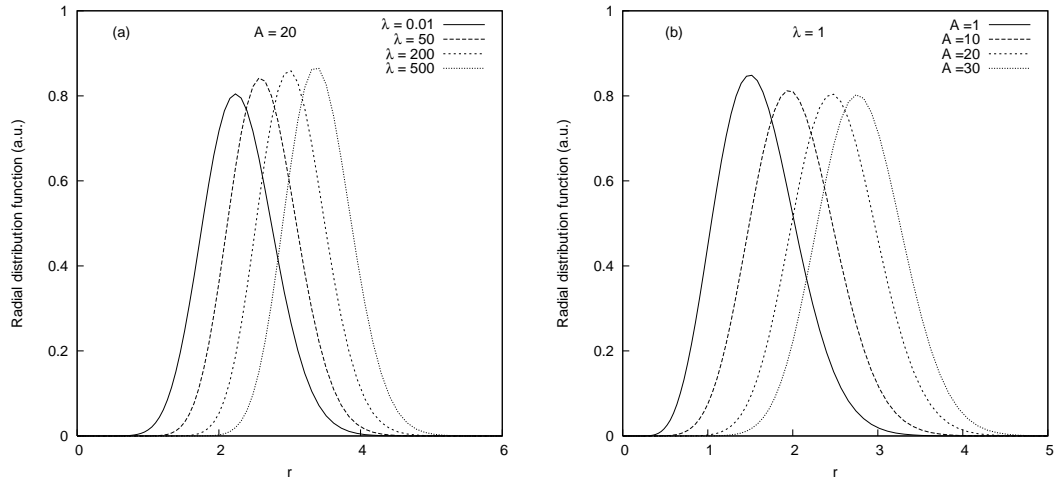


FIG. 3: Change in radial probability distribution function, $|rR_{n,\ell}|^2$, for the ground state of GSHO with λ and A . (a) $\lambda = 0.001, 50, 200$ and 500 at $A = 20$, (b) $A = 1, 10, 20, 30$ at $\lambda = 1$.

TABLE III: Calculated expectation values (in a.u.) for the GSHO for some selected values of λ for $\alpha = 4$ (left) and 6 (right). First two states belonging to $\ell = 0$ are presented. $A = 20$.

$\alpha = 4$				$\alpha = 6$			
λ	ℓ	$\langle r^{-1} \rangle$	$\langle r \rangle$	λ	ℓ	$\langle r^{-1} \rangle$	$\langle r \rangle$
1	0	0.455313939	2.30630576	1	0	0.456468262	2.300730227
		0.433586990	2.62193026			0.433801832	2.619954805
10	0	0.434300669	2.40340664	10	0	0.444230432	2.353215494
		0.409762190	2.72989436			0.415474164	2.697640059

IV. CONCLUSION

Discrete bound-state spectra of the GSHO are studied for the first time in detail by accurately calculating the eigenvalues, eigenfunctions, position expectation values and densities by means of the GPS method. The formalism is quite simple, computationally efficient, reliable and as illustrated, very accurate. Low as well as high states are calculated for arbitrary values of the interaction parameters covering weak and strong couplings with equal ease and accuracy. Only estimates of the upper and lower bounds of a few ground states have been reported so far in the literature; no direct results are available for the GSHO, not to speak of the highly accurate values. Thus we hope that our calculation of these hitherto unreported results would constitute a useful reference for future works on this system. In addition, the variation of eigenvalues and densities with respect to the potential parameters are also discussed.

Acknowledgments

AKR thanks Professors D. Neuhauser and S. I. Chu for encouragement, financial support and useful discussions. He thanks Dr. E. I. Proynov for helpful discussion. AKR acknowledges the warm hospitality provided by Univ. of California, Los angeles, CA, USA.

-
- [1] L. C. Detwiler and J. R. Klauder, Phys. Rev. D **11**, 1436 (1975).
 - [2] J. R. Klauder, Science **199**, 735 (1978).
 - [3] E. M. Harrell, Ann. Phys. (N. Y.) **105**, 379 (1977).

- [4] V. C. Aguilara-Navarro, G. A. Estévez and R. Guardiola, J. Math. Phys. **31**, 99 (1990).
- [5] V. C. Aguilara-Navarro and R. Guardiola, J. Math. Phys. **32**, 2135 (1991).
- [6] F. M. Fernández, Phys. Lett. A **160**, 511 (1991).
- [7] V. C. Aguilara-Navarro, F. M. Fernández, R. Guardiola and J. Ros, J. Phys. A **25**, 6379 (1992).
- [8] W. Solano-Torres, G. A. Estévez, F. M. Fernández and G. C. Groenenboom, J. Phys. A **25**, 3427 (1992).
- [9] E. Buendía, F. J. Gálvez and A. Puertas, J. Phys. A **28**, 6731 (1995).
- [10] R. L. Hall and N. Saad, Can. J. Phys. **73**, 493 (1995).
- [11] J. Trost and H. Friedrich, Phys. Lett. A **228**, 127 (1997).
- [12] R. L. Hall and N. Saad, J. Phys. A **31**, 963 (1998).
- [13] M. Znojil, Phys. Lett. A **255**, 1 (1999); *ibid.* **259**, 220 (1999).
- [14] O. Mustafa and M. Odeh, J. Phys. B **32**, 3055 (1999).
- [15] O. Mustafa and M. Odeh, J. Phys. A **33**, 5207 (2000).
- [16] J. P. Killingbeck, G. Jolicard, and A. Grosjean, J. Phys. A **34**, L367 (2001).
- [17] R. L. Hall, N. Saad and A. von Keviczky J. Math. Phys. **43**, 94 (2002)
- [18] A. K. Roy, Phys. Lett. A **321**, 231 (2004).
- [19] R. L. Hall, N. Saad and A. von Keviczky J. Math. Phys. **39**, 6345 (1998).
- [20] R. L. Hall and N. Saad, J. Phys. A **33**, 569 (2000).
- [21] R. L. Hall and N. Saad, J. Phys. A **33**, 5531 (2000).
- [22] R. L. Hall, N. Saad and A. von Keviczky J. Phys. A **34**, 1169 (2001).
- [23] N. Saad, R. L. Hall and A. von Keviczky J. Phys. A **36**, 487 (2003).
- [24] N. Saad, R. L. Hall and A. von Keviczky J. Math. Phys. **44**, 5021 (2003).
- [25] A. K. Roy, J. Phys. B **37**, 4369 (2004); *ibid.* **38**, 1591 (2005).
- [26] A. K. Roy, Int. J. Quant. Chem. **104**, 861 (2005).
- [27] A. K. Roy, Pramana-J. Phys. **65**, 1 (2005).
- [28] K. D. Sen and A. K. Roy, Phys. Lett. A **357**, 112 (2006).
- [29] B. L. Burrows, M. Cohen and T. Feldmann, J. Phys. A **20**, 889 (1987).